Neutron diffraction from liquid hydrogen bromide: Study of the orientational correlations

C. Andreani and F. Menzinger
Department of Physics University of Tor Vergata, Via della Ricerca Scientifica 11, 00172 Roma, Italy

M. A. Ricci
Department of Physics "E. Amaldi" University of Rome III, Via Segre 2, 00154 Roma, Italy

A. K. Soper and J. Dreyer
ISIS Facility, Rutherford Appleton Laboratory, Chilton, Didcot, Oxon, OX11 OQX United Kingdom
(Received 25 June 1993; revised manuscript received 13 October 1993)

The three partial structure factors of liquid hydrogen bromide along the coexistence curve have been measured by neutron diffraction using the isotopic substitution technique. The structure factors and corresponding pair correlation functions obtained suggest that it is an excellent approximation to regard the bromine atom as the center of mass of the hydrogen bromide molecule. The anisotropic terms in the intermolecular potential manifest themselves primarily by causing a significant degree of correlation between the orientations of neighboring molecules. In order to gauge the size of these orientational correlations an image reconstruction technique is employed. This analysis shows that there is a pronounced correlation between the *relative* orientations of neighboring molecules, but that there is not a strong directionality in the local coordination of any particular molecule. The results are discussed in relation to a previous experiment on hydrogen bromide which proposed the formation of hydrogen bonds in this liquid.

INTRODUCTION

Recently the site-site partial structure factors for liquid hydrogen iodide have been measured, using neutron diffraction with hydrogen isotope substitution.[1,2] This experiment was the first of several planned for the hydrogen-halide series, the purpose being to demonstrate the role of multipolar forces in generating orientational correlations in these liquids. The hydrogen halides are well suited for this study because the electronic overlap between molecules gives rise to a hard-core repulsion that is almost isotropic throughout the series, while the anisotropic interactions due to multipolar and polarization forces change monotonically down the series.[2] At one extreme of the hydrogen-halide series, hydrogen fluoride is expected to exhibit the greatest degree of orientational correlation, perhaps because the relatively low atomic number of the halide atom gives rise to the weakest isotropic repulsive forces and the strongest electrostatic ordering forces. At the other end of the series, hydrogen iodide is, because of its large atomic number, expected to show the weakest degree of orientational correlation. Therefore it is of some interest to look at the intermediate systems, liquid hydrogen chloride and liquid hydrogen bromide, to see the trend in the orientational structure with atomic number of the halide atom.

The neutron diffraction technique, with hydrogen isotope substitution, permits all three partial structure factors of the hydrogen-halide system to be extracted independently from one another. These partial structure factors are related by Fourier transform to the corresponding site-site pair correlation functions. In liquid hydrogen halides it is an excellent approximation to regard the halide atom as the center of mass. Consequently, the halide-halide structure factor is derived directly from the center of mass pair correlation function. The shape of the hydrogen-halide structure factor is then determined by the extent of orientational correlations between one molecule and the center of mass of a neighboring molecule, while the hydrogen-hydrogen structure factor is also sensitive to *relative* orientations between molecules.

Previous neutron diffraction work on liquid hydrogen bromide investigated only the deuterated compound.[3] This work yielded valuable information on the molecular geometry, but because of the close similarity in the neutron scattering lengths of deuterium and bromine, it was difficult to extract unambiguous information about specific site-site correlations from the composite structure factor and pair correlation function obtained. Previous work on hydrogen chloride[4] and hydrogen iodide[1] has demonstrated that the shape of the individual hydrogen-hydrogen, hydrogen-halide, and halide-halide correlations are quite distinct from one another and can only be properly determined if three isotopically substituted samples are available.

The present work describes a new neutron diffraction study of liquid hydrogen bromide with hydrogen isotope substitution. The experiment was run under the same reduced conditions ($T^* = T/T_c = 0.6$, where $T_c = 363$ K is the critical temperature) as the previous hydrogen

iodide experiment. In the following sections, the experiment and data analysis procedure are first described in detail. Then the measured atom-atom partial structure factors and site-site pair correlation functions are discussed in terms of the likely orientational correlations between neighboring molecules that they imply. To develop a more quantitative picture of these correlations an attempt is made to reconstruct the orientational pair correlation function $g(\mathbf{r}, \omega_1, \omega_2)$ using a method developed for modeling liquid hydrogen iodide.[2] Finally the results of this reconstruction are discussed in relation to previous data on the crystalline and liquid phases of HBr.

EXPERIMENTAL PROCEDURE AND DATA ANALYSIS

Measurements were performed with the SANDALS spectrometer at the ISIS spallation neutron source at the Rutherford Appleton Laboratory.[5] Samples of HBr and DBr (99.8% deuterated) gases were obtained from the Cambridge Isotope Laboratories and a mixture of $H_{0.48}D_{0.52}Br$ was prepared during the experiment by mixing the two pure gases in the correct proportions.

The three samples HBr, DBr, and $H_{0.481}D_{0.52}Br$ were contained in the same flat cell made of Ti-Zr alloy. This particular alloy scatters neutrons almost incoherently, and moreover has good corrosion resistance; so it does not distort the diffraction pattern significantly. The cell was 23 mm wide with an inner spacing of 2 mm and a wall thickness of 1 mm. The cell was in contact with a cold finger on the bottom of a closed cycle refrigerator. Two thermocouples were attached to the top and bottom of the cell to allow accurate measurements of the sample temperature. The thermal gradient across the sample cell was kept below 0.2 K by a radiation shield (thin aluminum foil) around the cell. Measurements were performed on three samples of the coexistent liquid at a temperature of (216.7±0.2) K and at a pressure of $\sim 2.4\times10^5$ Pa, where the number density is $\rho = 0.015$ molecules/Å^3. Since the saturated vapor pressure is 1.8×10^5 Pa, these conditions guaranteed that the liquid meniscus was well above the top of the cell during experiment.

Neutrons diffracted from the different samples HBr, DBr, and $H_{0.48}D_{0.52}Br$, empty container, vanadium, and background were recorded as a function of the neutron time of flight at the various detector scattering angles on SANDALS. The reproducibility of the measurements was checked by recording several runs, each of approximately 3 h duration, for each sample, and it was seen to be of the order of the statistical accuracy. Experimental corrections to the time-of-flight data were applied to account for background, multiple scattering, absorption, and empty container by the usual routines available on SANDALS.[6] The multiple scattering for the three samples was evaluated by a routine developed specially for flat plate samples to calculate the multiple scattering to all orders of scattering, within the isotropic scattering approximation.[7] The most severe multiple scattering contribution occurred for HBr and was estimated to be $\sim$ 7% over most of the Q range. (One advantage of pulsed neutrons here is that the neutron scattering cross section for hydrogen falls rapidly to one-quarter its nominal "bound" value with increasing neutron energy, so that the thickness of hydrogen-containing samples that can be tolerated at pulsed sources is generally greater than might be expected on the basis of the published bound cross section values.[8] The neutron energies used in this experiment ranged from 10 meV to as high as 30 eV.) The absolute differential cross sections were then obtained by comparison with the corrected vanadium spectrum at each scattering angle. These functions are plotted versus Q, the elastic momentum transfer, in Fig. 1 for one scattering angle for the three isotope samples. From this figure it can be concluded that in the high-Q region the inelastic contributions are almost negligible since the three cross sections oscillate around the expected $\sigma_s/4\pi$ value (see Table I). The inelastic scattering contribution to the cross sections is confined essentially to the Q region below 10 Å^{-1} for HBr and is almost undetectable in DBr. The confinement of the inelastic scattering in the low-Q region of the spectrum arises from the design of SANDALS, which has all its detectors concentrated at low scattering angles.

We now briefly review the formalism already used in Ref. 1 to describe the neutron scattering differential cross sections.

The procedure is to write the cross section per molecule, after experimental corrections, as

$$\left(\frac{d\sigma}{d\Omega}\right)_i = F_i^{\text{inter}}(Q) + F_i^{\text{intra}}(Q) + \frac{\sigma_{s,i}}{4\pi}[1 + P_i(Q)] , \tag{1}$$

where $F_i^{\text{inter}}(Q)$ and $F_i^{\text{intra}}(Q)$ are the inter- and intramolecular interference scattering functions, respectively, $P_i(Q)$ is the inelasticity contribution to the self-scattering of the ith sample (i = HBr, DBr, $H_{0.48}D_{0.52}Br$), and $\sigma_{s,i}$ is its total scattering cross section. For a given sample the total $F(Q)$ function is given in terms of the partial structure factors $S_{\alpha\beta}(Q)$ as

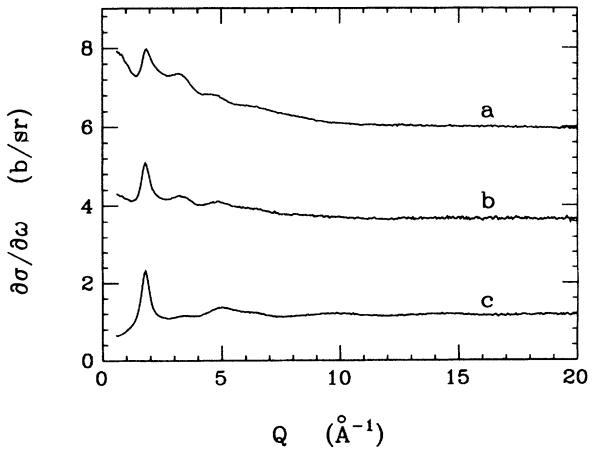

FIG. 1. Total differential scattering cross section in the units of b/sr/molecule for one detector (2θ = 20.13°) as a function of the momentum transfer Q for the three measured samples (a =HBr, b =$H_{0.48}D_{0.52}Br$, c =DBr).

TABLE I. Values of coherent scattering length b_c and coherent and total cross sections σ_c and σ_s, for atoms H, Br, and V (Ref. 8).

Element	Mass number	Natural abundance (%)	b_c (fm)	σ_c (b)	σ_s (b)
H	1	99.985	−3.741	1.758	82.03
	2	0.0150	6.671	5.592	7.64
Br	nat	100.00	6.795	5.800	5.900
V	nat	100.00	−0.382	0.018	5.10

$$F(Q) = F^{\text{inter}}(Q) + F^{\text{intra}}(Q) = \sum_{\alpha\beta} b_\alpha b_\beta [S_{\alpha\beta}(Q) - \delta_{\alpha\beta}] \,, \tag{2}$$

with b_α the scattering length for species α (see Table I). The $S_{\alpha\beta}(Q)$ functions include both inter- and intramolecular contributions. In our case the modulation due to the DBr molecule in the high-Q region is weighted, from Eq. (2), with a larger amplitude ($2b_{\text{Br}}b_{\text{D}} = 0.906 \times 10^{-24}$ cm^2) as compared to the weighting for HBr ($2b_{\text{Br}}b_{\text{H}} = -0.508 \times 10^{-24}$ cm^2) and for $H_{0.48}D_{0.52}Br$ ($2b_{\text{Br}}b_{\text{HD}} = 0.227 \times 10^{-24}$ cm^2).

To extract the structural information on the liquid, a further correction has to be applied to the data of Fig. 1 in order to subtract the inelastic atomic self-scattering contribution $P_i(Q)$. There is currently no rigorous formalism for coping with the inelastic scattering from hydrogen in diffraction measurements. Therefore we proceeded with a two track approach, which allowed us to make an internal check on the final interference functions obtained. The first procedure has been described in detail for a recent experiment on dimethyl sulphoxide in aqueous solution[9] and is hereafter named P1. This procedure consists of representing the inelastic self-scattering with a polynomial functional form. The correction is applied to the total, inter- plus intramolecular, differential cross sections of Fig. 1, at each scattering angle. Good agreement among the $F(Q)$ functions from different scattering angles verifies the reliability of the correction. The second approach (hereafter named P2) involves estimating the entire single molecule scattering contribution to the diffraction data. The P2 method is described in Ref. 10, and has been tested in the case of a gaseous system of water molecules. In the present case a simple analytic function was fitted to the DBr data of Fig. 1 with

$$\begin{aligned} &F^{\text{intra}}(Q) + \frac{\sigma_s}{4\pi}[1 + P_{\text{DBr}}(Q)] \\ &\quad = 2b_{\text{D}}b_{\text{Br}} \frac{\sin QR}{QR} \exp(-\frac{1}{2}\langle u^2_{\text{DBr}}\rangle Q^2) \\ &\qquad + A + B\exp[-(CQ)^D] \,, \end{aligned} \tag{3}$$

where R is the intramolecular bond length, $\langle u^2_{\text{DBr}}\rangle$ is the averaged mean square amplitude of the atomic motion, and A, B, C, and D are fitting parameters. In Fig. 2 the experimental $(\frac{d\sigma}{d\Omega})$ of DBr at one scattering angle, in the range $5 - 16$ Å^{-1}, is plotted as a function of Q together with its best fit. The same fit has been performed for each angle, and the different R and $\langle u^2_{\text{DBr}}\rangle$ parameters were found to be in excellent agreement with each other. The DBr molecular parameters, averaged over the angles, are $R = (1.446 \pm 0.002)$ Å and $\langle u^2_{\text{DBr}}\rangle = (7.1 \pm 0.6) \times 10^{-3}$ Å^2. We observe that the R value of the liquid phase is in excellent agreement with previous neutron scattering data on liquid DBr, for which an intramolecular distance of 1.443 Åwas obtained.[3] The R value is slightly larger than the quoted value for the gas phase, i.e., $R_{\text{gas}} = 1.414$ Å,[11] even if one allows for the anharmonicity of the zero point vibration. Furthermore, as with deuterium iodide, the fitted $\langle u^2_{\text{DBr}}\rangle$, representing an *effective* Debye-Waller amplitude, is larger than the value 4.35×10^{-3} Å^2 obtained from vibrational frequency.[12] Figure 3 shows the $(\frac{d\sigma}{d\Omega})$ function of Fig. 2 in the overall Q range together with the

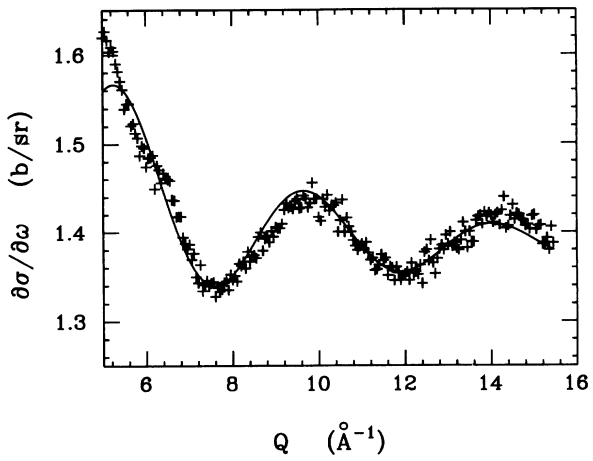

FIG. 2. Total differential scattering cross section per molecule for DBr ($2\theta = 20.13°$) in the range in which the intramolecular cross section is largely predominant. Experimental points (+++); best fit using Eq. (3) in the text (solid line).

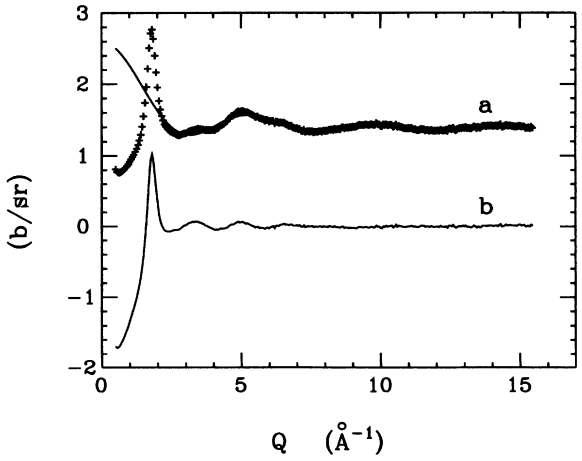

FIG. 3. (a) Total differential scattering cross section per molecule for DBr ($2\theta = 20.13°$) (+++) and intramolecular fitted cross section (solid line); (b) interference scattering function $F^{\text{inter}}_{\text{DBr}}(Q)$.

fitted intramolecular contribution and the corresponding $F^{\text{inter}}(Q)$ function. The same analytical function of Eq. (3) was applied to correct HBr and $H_{0.48}D_{0.52}Br$ cross sections for the inelastic contributions, keeping the R distance fitted for DBr fixed and scaling the Debye-Waller factor according to the lighter mass of each sample. The fits were independently performed at each scattering angle. The function given by Eq. (3) was found to account satisfactorily for the self-scattering contribution in the range $0 - 15$ Å^{-1}.

A comment on Eq. (3) is that the last term, the stretched exponential function, successfully fits the rising slope of the low-Q range in the hydrogen-containing samples, that is, in the region where the inelastic contribution and errors in the multiple scattering corrections to the cross section are more severe. Parameter A approximately represents the appropriate $\frac{\sigma_s}{4\pi}$ value, whereas $A + B$ obey the constraint that $F^{\text{inter}}(Q)$ approach the correct limiting value as $Q \to 0$, that is, in the case of a liquid with $\rho\chi K_B T << 1$:

$$F^{\text{inter}}(0) = -\left[\sum_\alpha b_\alpha\right]^2 . \tag{4}$$

After subtraction of the inelastic contributions for each scattering angle a good superposition of the $F^{\text{inter}}(Q)$ signal was obtained for six out of the ten angles. Merged $F^{\text{inter}}(Q)$ functions from these six angles were then derived for both P1 and P2 procedures and combined linearly to give the three intermolecular partial structure factors $S^{\text{inter}}_{\text{HH}}(Q)$, $S^{\text{inter}}_{\text{HBr}}(Q)$, and $S^{\text{inter}}_{\text{BrBr}}(Q)$ as

$$S^{\text{inter}}_{\alpha\beta}(Q) = H_{\alpha\beta}F^{\text{inter}}_{\text{DBr}}(Q) + L_{\alpha\beta}F^{\text{inter}}_{\text{HBr}}(Q) + M_{\alpha\beta}F^{\text{inter}}_{\text{HDBr}}(Q) . \tag{5}$$

The weighting coefficients $H_{\alpha\beta}$, $L_{\alpha\beta}$, and $M_{\alpha\beta}$ for our experiment are listed in Table II.

The $S_{\alpha\beta}(Q)$ functions derived from procedures P1 and P2 compared well with each other. For the two partials $S^{\text{inter}}_{\text{HBr}}(Q)$ and $S^{\text{inter}}_{\text{BrBr}}(Q)$, the agreement between different procedures was better than the statistical errors. However, for the $S^{\text{inter}}_{\text{HH}}(Q)$ function (see Fig. 4), although the results of the two methods show the same qualitative features in terms of peak positions and overall shape, a difference in the absolute signal level does occur in the low-Q region. Subsequent Fourier analysis to the pair correlation function for these two results suggested that this discrepency was in fact caused by differences in the ways the low-Q part of the incoherent differential cross section is represented in the two methods. To understand how this was established, we will now outline the method of performing Fourier transforms used in this experiment and elsewhere.

The Fourier transform of neutron structure data on liquids, $S(Q)$, to the pair correlation function $g(r)$ is bedeviled by a number of problems associated with the statistical noise and residual systematic errors that occur both in accumulating the data itself and in the subsequent data analysis. For pulsed neutron work the truncation of the data at finite Q is rarely a difficulty in itself, because the Q range available is normally fully adequate. However, the combination of statistical noise and finite Q *is* important because even when the structure factor signal itself has gone to zero at the large-Q limit, the noise term is never zero. If a direct Fourier inversion is performed on noisy data, large amplitude truncation ripples are likely to occur in the transformed result just from the *noise* in the the structure data. For these reasons one of us has argued[13,14,2] that the correct way to analyze $S(Q)$ data to $g(r)$ is *not* to perform a direct Fourier transform on the data, but instead apply a tight restriction on the form $g(r)$ can take. In particular we should insist that the most reasonable $g(r)$ function is one which is as smooth as possible but nonetheless consistent with the data, within the known measuring errors. At the same time we should insist that any derived $g(r)$ function be positive definite, that $g(r)$ be zero within a sensible hard core radius, and that the $Q = 0$ limit to $S(Q)$ be satisfied by the derived $g(r)$, where this limit is known. In this way we not only derive a sensible $g(r)$, but also gauge some idea of the systematic errors introduced by the measuring process.[13]

In the present work we have adopted the minimum noise (min) procedure to extract the pair correlation functions.[14,2] One of the results of this analysis is an estimate of the systematic error in the data, $E(Q)$, which would otherwise give rise to unphysical behavior in the derived pair correlation function.[13] The difference between the measured data and $E(Q)$ is then a corrected version of the data without those systematic errors. For

TABLE II. Intermolecular partial structure factor weighting coefficients for Eq. (5).

	$H_{\alpha\beta}$	$L_{\alpha\beta}$	$M_{\alpha\beta}$
S_{BrBr}	−0.261	0.429	2.001
S_{HH}	1.921	1.774	−3.695
S_{HBr}	0.293	−1.090	0.797

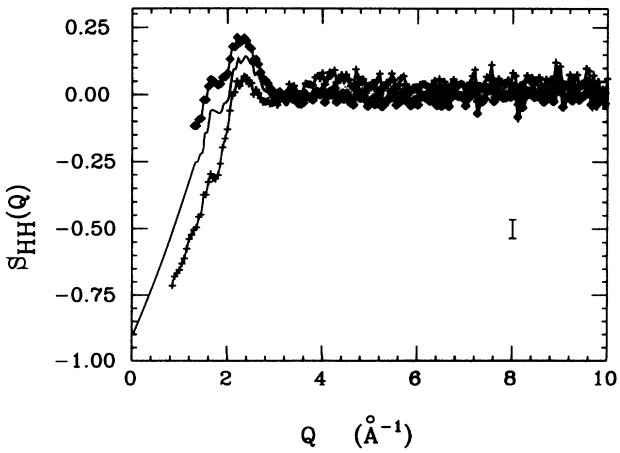

FIG. 4. Hydrogen-hydrogen experimental partial structure factor $S^{\text{inter}}_{\text{HH}}(Q)$, according to Eq. (5), derived with procedure P1 (diamonds) and procedure P2 (+++) (see text). Solid line is $S^{\text{min}}_{\text{HH}}(Q)$. The typical error bar is also shown in the figure.

the two "measured" HH functions shown in Fig. 4 it was found that although the original version of the data have marked discrepencies at low Q, these differences could be resolved entirely as coming from systematic error introduced in the process of removing the inelastic scattering. The two corrected versions of the HH data, here labeled $S_{HH}^{min}(Q)$, overlapped one another almost completely, and so only one of them is shown as the line in Fig. 4. At the same time we concluded that in spite of differences between the two methods for removing the effects of inelasticity, the underlying structure factors and pair correlation functions that were extracted were robust against

TABLE III. Intermolecular partial structure factors, $S_{HH}^{min}(Q)$, $S_{HBr}^{min}(Q)$, and $S_{BrBr}^{min}(Q)$, for liquid HBr at $T = 216.7$ K.

Q (Å^{-1})	$S_{HBr}^{min}(Q)$	$S_{BrBr}^{min}(Q)$	$S_{HH}^{min}(Q)$	Q (Å^{-1})	$S_{HBr}^{min}(Q)$	$S_{BrBr}^{min}(Q)$	$S_{HH}^{min}(Q)$
0.050	-0.881	-0.874	-0.878	5.150	0.015	0.050	0.002
0.150	-0.865	-0.819	-0.839	5.250	0.016	0.036	0.002
0.250	-0.876	-0.805	-0.801	5.350	0.013	0.013	0.002
0.350	-0.865	-0.786	-0.746	5.450	0.010	-0.006	0.002
0.450	-0.854	-0.769	-0.708	5.550	0.006	-0.016	0.002
0.550	-0.834	-0.750	-0.657	5.650	0.001	-0.024	0.001
0.650	-0.815	-0.738	-0.608	5.750	-0.002	-0.029	0.000
0.750	-0.769	-0.717	-0.559	5.850	-0.005	-0.027	-0.001
0.850	-0.701	-0.743	-0.508	5.950	-0.006	-0.019	-0.001
0.950	-0.605	-0.798	-0.453	6.050	-0.006	-0.017	-0.001
1.050	-0.502	-0.831	-0.403	6.150	-0.006	-0.016	-0.001
1.150	-0.406	-0.850	-0.347	6.250	-0.005	-0.010	0.000
1.250	-0.311	-0.851	-0.290	6.350	-0.004	-0.002	0.000
1.350	-0.207	-0.765	-0.250	6.450	-0.003	0.010	0.000
1.450	-0.119	-0.616	-0.214	6.550	-0.002	0.019	0.000
1.550	-0.007	-0.303	-0.142	6.650	-0.002	0.022	0.000
1.650	0.114	0.235	-0.080	6.750	-0.002	0.017	0.000
1.750	0.208	0.976	-0.058	6.850	-0.001	0.011	0.000
1.850	0.160	1.289	-0.063	6.950	-0.001	0.008	0.000
1.950	0.022	0.931	-0.039	7.050	0.000	0.005	0.000
2.050	-0.069	0.423	0.024	7.150	0.001	0.002	0.000
2.150	-0.090	0.048	0.088	7.250	0.002	-0.002	-0.001
2.250	-0.065	-0.147	0.124	7.350	0.002	-0.008	0.000
2.350	-0.024	-0.268	0.132	7.450	0.003	-0.014	0.000
2.450	0.019	-0.324	0.120	7.550	0.002	-0.015	0.000
2.550	0.057	-0.342	0.093	7.650	0.002	-0.011	0.000
2.650	0.079	-0.327	0.058	7.750	0.002	-0.008	0.000
2.750	0.089	-0.290	0.025	7.850	0.001	-0.005	0.000
2.850	0.083	-0.207	-0.001	7.950	0.001	-0.002	0.000
2.950	0.063	-0.105	-0.019	8.050	0.001	0.003	0.000
3.050	0.037	-0.010	-0.027	8.150	0.000	0.008	0.000
3.150	0.003	0.094	-0.027	8.250	0.000	0.011	0.000
3.250	-0.025	0.167	-0.024	8.350	-0.001	0.013	0.000
3.350	-0.041	0.204	-0.022	8.450	-0.001	0.011	0.000
3.450	-0.042	0.205	-0.022	8.550	-0.001	0.006	0.000
3.550	-0.037	0.184	-0.020	8.650	-0.001	0.000	0.000
3.650	-0.029	0.130	-0.016	8.750	-0.001	-0.005	0.000
3.750	-0.019	0.055	-0.009	8.850	-0.001	-0.007	0.000
3.850	-0.010	-0.009	-0.003	8.950	-0.001	-0.008	0.000
3.950	-0.001	-0.073	0.002	9.050	-0.001	-0.006	0.000
4.050	0.003	-0.101	0.005	9.150	0.000	-0.005	0.000
4.150	0.004	-0.114	0.006	9.250	0.000	-0.003	0.000
4.250	0.001	-0.109	0.006	9.350	0.000	-0.001	0.000
4.350	-0.003	-0.087	0.005	9.450	0.000	0.000	0.000
4.450	-0.008	-0.063	0.003	9.550	0.000	0.000	0.000
4.550	-0.010	-0.030	0.001	9.650	0.000	0.000	0.000
4.650	-0.010	0.003	0.000	9.750	0.000	0.001	0.000
4.750	-0.006	0.031	0.000	9.850	0.000	0.004	0.000
4.850	0.001	0.053	0.000	9.950	0.000	0.005	0.000
4.950	0.007	0.062	0.000	10.050	0.000	0.005	0.000
5.050	0.013	0.061	0.001				

possible distortion introduced by the correction procedure.

For these reasons, in the subsequent discussion we will use only the corrected data $S^{\min}_{\alpha\beta}(Q)$ to represent the measured structure of the liquid and to perform all the necessary comparisons with models. These functions are listed in Table III and displayed in Fig. 5.

In Fig. 5(a) the center of mass partial structure function $S^{\min}_{\mathrm{BrBr}}(Q)$ is reported together with the corresponding quantity for a Lennard-Jones (LJ) fluid obtained by molecular-dynamics (MD) simulation at $\rho^* = 0.86$ and $T^* = 0.76$. These reduced parameters for the simulation were chosen according to the corresponding state principle, which gives for hydrogen bromide the effective LJ parameters $\sigma = 3.86$ Å and $\varepsilon/K_B = 288$ K with $T_c = 1.26\varepsilon/K_B$ and $P_c = 12.2 \times 10^{-8}\varepsilon/\sigma^3$. The critical state parameters can be found in Ref. 12. The agreement is excellent and serves to verify the assumption that $S^{\min}_{\mathrm{BrBr}}(Q) \sim S_{cc}(Q)$, the structure factor of the molecular mass centers. In Figs. 5(b) and 5(c) the HBr and HH structure factors are compared to functions derived for an ideal isotropic hydrogen-bromide liquid, where orientational correlations are neglected altogether.[1] The latter is in the following referred to as the uncorrrelated model (UM). In this case the $S_{cc}(Q)$ was used to reconstruct the other two partial structure factors for the uncorrelated model as

$$S^{(\mathrm{UM})}_{\mathrm{HBr}}(Q) = [S_{cc}(Q) - 1]\frac{\sin(QR)}{QR} , \tag{6}$$

$$S^{(\mathrm{UM})}_{\mathrm{HH}}(Q) = [S_{cc}(Q) - 1]\left(\frac{\sin(QR)}{QR}\right)^2 , \tag{7}$$

where $R = 1.446$ Å.

Comparison of these uncorrelated model functions with those measured with neutrons shows substantial discrepancies, unlike the case of the BrBr structure factor. Therefore even without further analysis there is already clear evidence for a high degree of orientational correlation in this liquid. In Figs. 6(a), 6(b), and 6(c) the intermolecular pair distribution functions $g_{\alpha\beta}(r)$ are plotted together with the similar functions derived by Fourier transforming the corresponding $S^{(\mathrm{UM})}_{\alpha\beta}(Q)$ functions.

ORIENTATIONAL CORRELATION RECONSTRUCTION

In analyzing diffraction data from molecular liquids it is common practice to derive only the site-site pair correlation functions and compare these quantities with similar functions derived from a computer simulation experiment. However, in recent work on liquid hydrogen iodide, an attempt was made to go beyond the usual data analysis by deriving an orientational pair correlation function $g(\mathbf{r}, \omega_1, \omega_2)$ which was consistent with the diffraction data set.[2] The function $g(\mathbf{r}, \omega_1, \omega_2)$ is more fundamental than the site-site correlation functions since it contains all the information needed to define the intermolecular potential, at least in the pair approximation.[15] Both correlation functions can be expanded as a series of spherical harmonics and the two expansions are related by a common set of coefficients, $H(l_1 l_2 l; Q)$, which in turn are related by an inverse Hankel transform to the real space expansion coefficients $h(l_1 l_2 l; r)$.[15] The difference in the

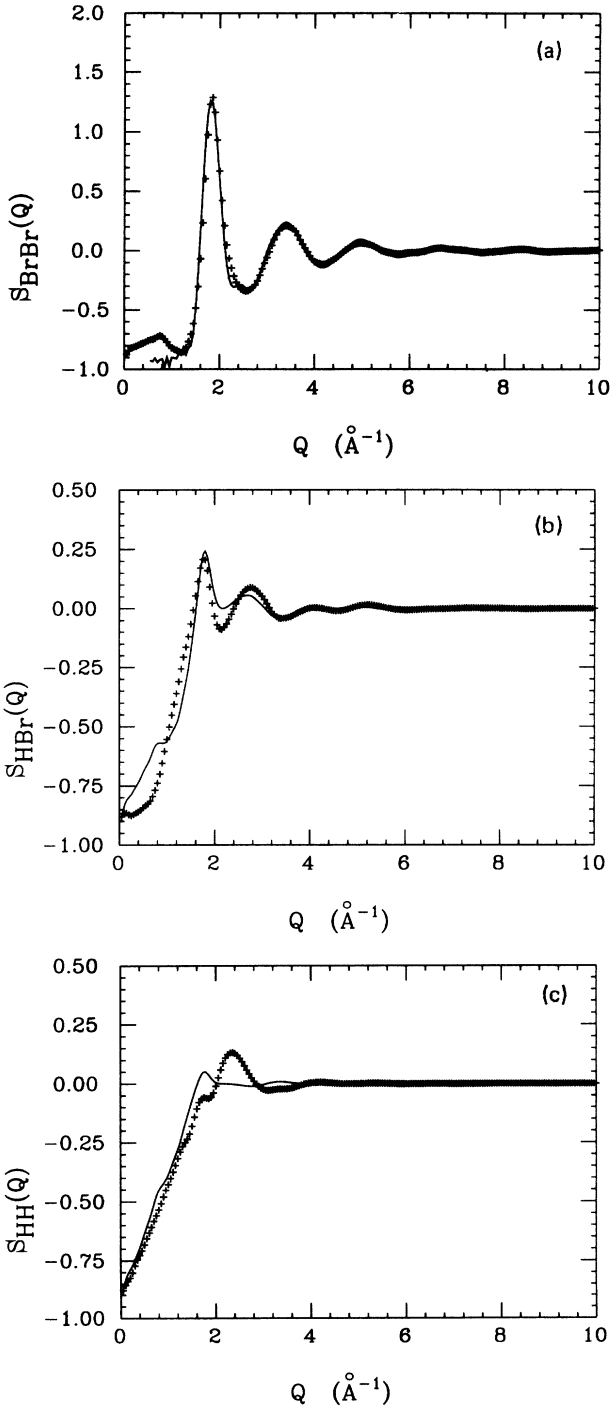

FIG. 5. (a) Bromine-bromine experimental partial structure factor $S^{\min}_{\mathrm{BrBr}}(Q)$ (+++), determined from Eq. (5); structure factor of a LJ fluid derived by MD (solid line). (b) Hydrogen-bromine experimental partial structure factor $S^{\min}_{\mathrm{HBr}}(Q)$ (+++) and the prediction of the uncorrelated model, UM (solid line). (c) Same as (b) for hydrogen-hydrogen partial structure factor $S^{\min}_{\mathrm{HH}}(Q)$.

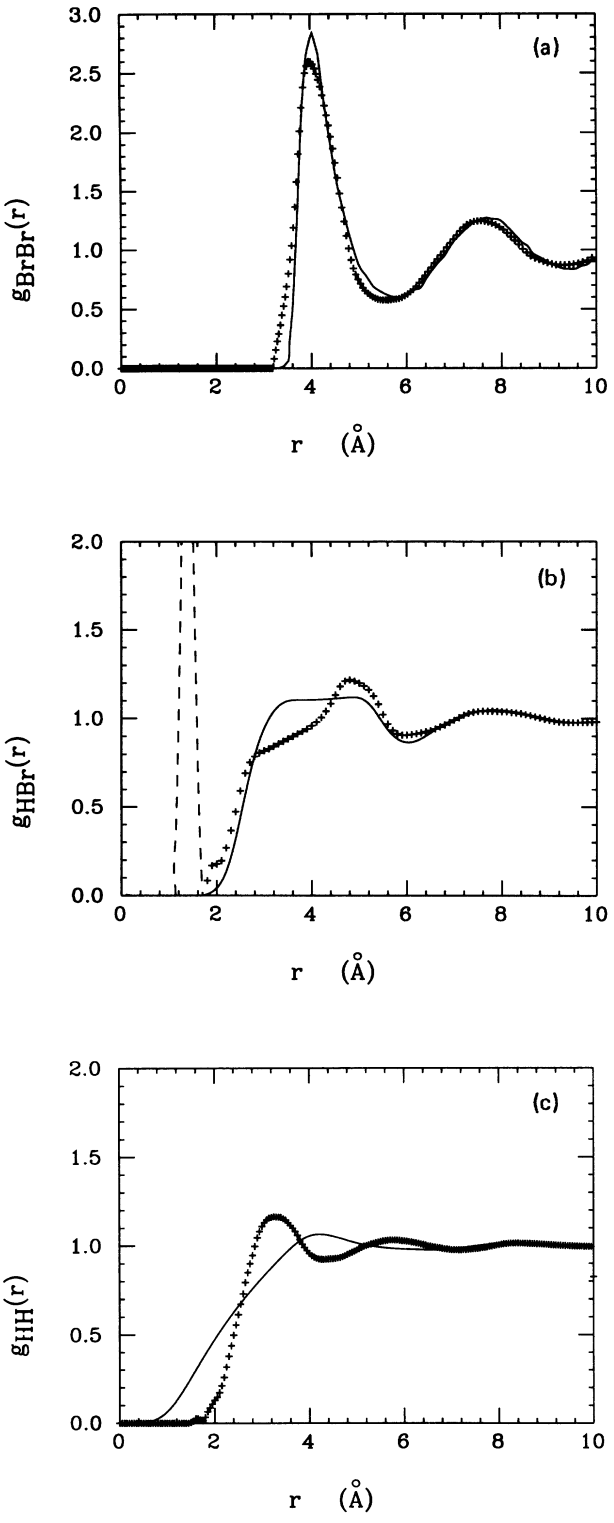

FIG. 6. (a) Bromine-bromine partial pair distribution function obtained from the min code (+++), compared with the Fourier inversion of the MD results from a LJ fluid (solid line) of Fig. 5(a). (b) Hydrogen-bromine intermolecular partial pair distribution function (+++), compared with the Fourier inversion of the UM from MD results from Eq. (6) (solid line); the dashed line represents the intramolecular contribution. (c) Same as (b) for the hydrogen-hydrogen partial pair correlation function.

two expansions is that certain closure rules are applied to the site-site expansion which limit the choice of coefficients that the experiment can access. In practice, for diatomic molecules, this limitation does not appear to be too severe. The underlying theme of the work described in Ref. 2 for hydrogen iodide was to determine the *minimum* amount of structure in the orientational pair correlation function which is needed to fit the data, while at the same time trying to ensure that this correlation function was everywhere positive.

A simple simulation of $g(\mathbf{r},\omega_1,\omega_2)$ is impractical because of the very large phase space needed to define this function completely. The spherical harmonic expansion offers a practical route to obtaining this function approximately from the data because it is an extremely compact representation in which molecular symmetry is built into the calculation from the beginning. There is some sacrifice in accuracy in using this expansion in regions where the orientational correlations are strong, such as the region of molecular contact for diatomic molecules, since then a very large number of terms are required to keep the simulated orientational correlation function always positive, and with typical present day computing power the calculation becomes inefficient with more than about 100 coefficients.

The reconstruction method has already been described in detail in Ref. 2 and so will not be repeated here. Expansions with $l_{\max} = 4$ and $l_{\max} = 6$ were carried out and found to give fits of similar quality. Orientational correlation functions derived from these two fits had essentially the same features. The results of this method for the present data are shown in Fig. 7, for $l_{\max} = 4$. The indices of the basis functions for the spherical harmonic expansion required to generate Fig. 7 are the same as those listed in Ref. 2.

One of the remarkable features to emerge from this reconstruction is the great propensity for near-neighbor molecules to lie at roughly 45° to each other over quite a wide range of directions in the laboratory axis system. For laboratory θ_L values up to $0° - 135°$ this occurs with the hydrogen atoms closer on the average to each other than the bromine atoms. This result can already be inferred from inspection of the site-site correlations shown in Figs. 6(a) and 6(c), where it appears that the minimum approach distance for the hydrogen atoms is smaller than the corresponding quantity for bromine atoms. Perhaps less obvious from the site-site correlations is the fact that for laboratory θ_L values greater than 90° some hydrogens also point away from the bromine and indeed for $\theta_L = 180°$ the majority of molecular dipoles are roughly antiparallel, a result which was also seen in the case of hydrogen iodide.[2]

When viewing these maps, Fig. 7, it is important to bear in mind that they are *density* maps and not number maps. The actual *percentage* of molecules in any particular configuration can only be estimated after taking account of the effects of solid angle subtended in different directions from the central molecule. The 45° configurations are found over a broad range of directions, including the case where $\theta_L = 90°$. Such directions therefore represent a large fraction of the available solid angle for

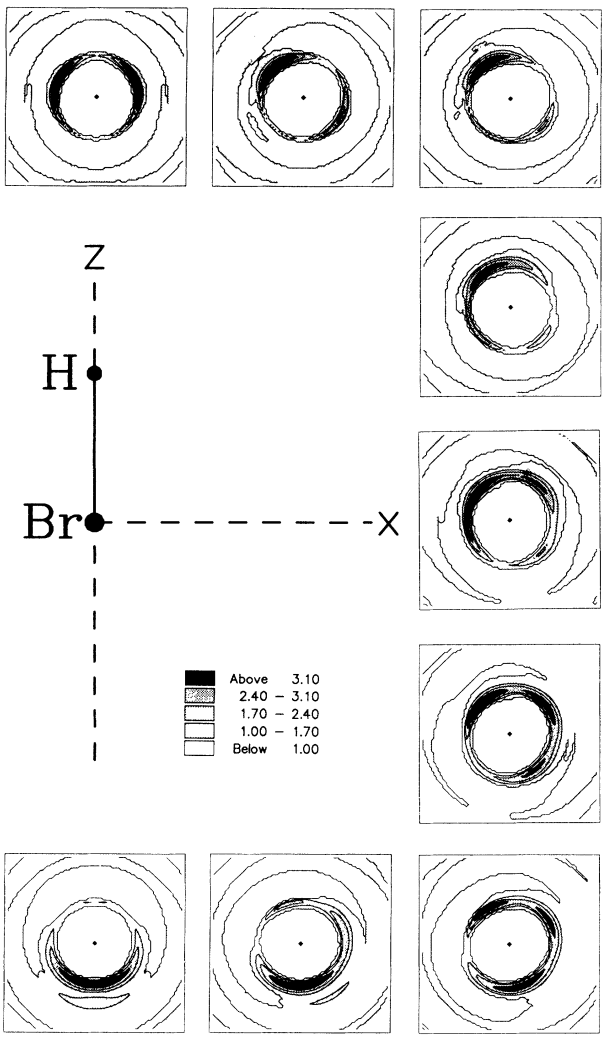

FIG. 7. Density maps of the angular pair correlation function between pairs of hydrogen-bromide molecules in the liquid state. A central molecule, molecule 1, is held fixed with its bromine atom at the origin of the laboratory coordinate system and with its hydrogen atom pointing along the positive z axis. Different directions away from this molecule are characterized by the value of θ_L, which is the angle made by molecular center-center vector with the z axis. The position of each map in the diagram, relative to the displayed coordinate system, corresponds closely to the actual value of θ_L for that map. Thus proceeding clockwise from the top the maps are shown for the different directions θ_L = 0°, 27°, 45°, 63°, 90°, 117°, 135°, 153°, and 180°. The maps are displayed on a square 20 Å× 20 Å. In each map the pair correlation function is shown as a function of the distance of a second molecule, molecule 2, from molecule 1 (central black dot). The angular variation of the intensity in each map corresponds to molecule 2 pointing in different directions in the x-z plane of the coordinate system relative to molecule 1. Dark regions in each map correspond to areas of enhanced density. For clarity, only values of the correlation function greater than unity are shown.

HBr molecules coordinating the central molecule. On the other hand the antiparallel configurations occur in directions close to the Br-H axis ($\theta_L \approx 180°$), and so the solid angle available for these configurations is much smaller. Therefore the relative number of molecules in this antiparallel configuration is probably quite small. Nonetheless it is interesting to note that there are rather few parallel configurations in evidence for both $\theta_L = 0°$ and $\theta_L = 180°$. This must be a direct consequence of there being a minimum in $g_{\mathrm{HH}}(r)$ at a position close to that of the main peak in BrBr (center of mass) correlation.

DISCUSSION

The good agreement of the BrBr structure factor and pair correlation function of Figs. 5(a) and 6(a) with the corresponding functions of a monoatomic LJ liquid at the same reduced temperature confirms that the anisotropic terms in the intermolecular potential of hydrogen bromide do not greatly influence the correlations between centers of mass of different hydrogen bromide molecules. However, comparison of the measured HBr and HH pair correlation functions with those derived from the uncorrelated model, Figs. 6(b) and 6(c), shows that there is a strong correlation between the orientation of neighboring molecules' axes. There may also be some correlation between the center of one molecule and the orientation of a neighboring molecule's axis. In particular we observe that the first peak in the HH pair correlation occurs at 3.2 Å, Fig. 6(c), and at a much shorter distance than the average molecular center distance of 4.0 Å, Fig. 6(a). Indeed the distance of 4.0 Å is close to the first *minimum* in the HH function. Therefore even at this simple level of interpretation there is strong evidence from the diffraction data that hydrogen-bromide molecules in the low-temperature liquid do *not* line up with their dipole moments parallel. If there really were a high degree of parallel alignment between molecules then the HH near-neighbor distance would have to correspond closely to that of the BrBr distance. Instead we find a minimum in the HH correlation at this distance. Spherical harmonic analyisis of the the partial structure factors, Fig. 7, indicates that the majority of molecules are lying in a broadband with their dipoles at $\sim 45°$ to one another.

There is also some indication of roughly antiparallel configurations in the maps of the orientational correlation function, Fig. 7, although one has to be cautious about overemphasizing these, since the maps are density maps, not number maps. Given the expected nature of the multipole interactions between neighboring molecules this second result appears to be counterintuitive. However, it is worth noting that exactly the same situation occurs in the high-temperature crystalline phase of hydrogen bromide, where disorder causes the HBr molecules to adopt one of 12 possible directions, more or less at random.[16] One of these directions is with the dipoles in the antiparallel configuration. Moreover, a significant degree of antiparallel correlation was also observed in liquid hydrogen iodide.[2] It is our view that a full resolution of this controversial result can only be achieved via a de-

tailed computer study of liquid hydrogen bromide, using a intermolecular potential which correctly represents the dipole, quadrupole, and polarizability forces. A further diffraction study of the high-temperature crystalline phase, similar to the one undertaken here on the liquid, might also yield valuable insight on whether these correlation effects transfer from liquid to the solid.

It is clear therefore that structural results from the liquid as established here will have important implications for the intermolecular potential for hydrogen bromide. A related question which is frequently discussed is the extent to which hydrogen halides should be regarded as "hydrogen bonded" liquids. Although there is no formal definition of the term "hydrogen bond," it generally refers to the strong directionality which occurs in some hydrogen-containing liquids (water is probably the best known example) in which the hydrogen on one molecule points in a particular direction towards another molecule. This hydrogen bond is accompanied by a characteristic signal in the partial structure factors. For example from the three site-site pair distribution functions in water, HH, OH, and OO,[17] it is possible to show that the local water coordination is roughly tetrahedral, with a large fraction of coordinating molecules pointing in particular directions relative a molecule at the origin. This hydrogen bonding is accompanied by a very distinct peak at ~ 1.9 Å in the OH pair correlation function in liquid water. Therefore it is interesting to establish whether such directionality exists in liquid hydrogen bromide as well.

In a previous paper concerning a neutron diffraction measurement of liquid deuterium bromide it was suggested that the presence of a small peak in the total pair correlation function, occurring at about 3.1 Å, was the fingerprint of a weak hydrogen bond in this system.[3] From the present measurements one can confirm the presence of a rather broad peak in the total $g(r)$ function around the same r value. In Fig. 8 the function $[g^{\mathrm{av}}(r) - 1]r$ is reported, where $g^{\mathrm{av}}(r)$ is the neutron weighted sum of the partial pair correlation functions, equivalent to pure deuterium bromide. The latter was obtained by summing the $g_{\alpha\beta}(r)$ of Fig. 6 with the appropriate weights:

$$g^{\mathrm{av}}(r) = 0.254 g_{\mathrm{BrBr}}(r) + 0.500 g_{\mathrm{BrH}}(r) + 0.246 g_{\mathrm{HH}}(r) \,. \tag{8}$$

We indeed observe a clear shoulder in this function between 2.5 and 3.1 Å associated with features at 2.6 Å and at 3.0 Å in the BrH and HH pair correlation functions respectively [see Figs. 6(b) and 6(c)]. Since these latter two features have already been seen to be a direct consequence of pronounced orientational correlations between molecules, it is tempting to suppose that this peak indicates the presence of a hydrogen bond in hydrogen bromide. However, finding this peak has to be considered in conjunction with the results of Fig. 7 where, although strong orientational correlations are certainly present, there is not a strong *directionality* in this correlation: The orientational correlations occur in all directions away from the molecule at the origin. The defining characteristic of hydrogen bonding, if there is one at all, is that the hydrogen of a neighboring molecule must point in a certain direction towards a molecule at the origin. The absence of a definite low-r peak in the HBr pair correlation function, Fig. 6(b), and the maps of $g(\mathbf{r}, \omega_1, \omega_2)$ in Fig. 7 argue against any significant degree of hydrogen bonding in this liquid.

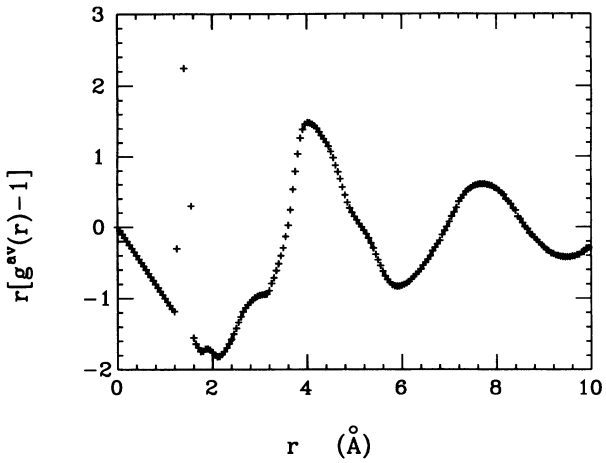

FIG. 8. The function $r[g^{\mathrm{av}}(r) - 1]$, where $g^{\mathrm{av}}(r)$ is defined by Eq. (8), as obtained from the experimental results given in Fig. 6. The peak at about 1.4 Åis the intramolecular HBr signal.

CONCLUSIONS

The data on liquid hydrogen bromide presented in this paper show that a wealth of information on the local coordination in a liquid can be extracted from a carefully executed neutron diffraction experiment, especially if hydrogen isotope substitution is exploited to separate out the site-site partial structure factors. The present data show a pronounced degree of orientational correlation between neighboring hydrogen bromide molecules, which does not fit into a simple picture of interacting dipoles and quadrupoles. A previous claim for the existence of hydrogen bond formation in liquid hydrogen bromide has been looked at carefully in the light of the present results. If hydrogen bonding does occur at all, it is certainly much weaker than that which occurs in liquid water where the hydrogen bond has a clear signature in the equivalent site-site pair correlation functions.[17] The original claim for hydrogen bonding in hydrogen bromide was made on the basis of neutron diffraction results performed on liquid DBr (Ref. 3) alone, which provided only the total weighted $g^{\mathrm{av}}(r)$ function, and because deuterium and bromine have almost identical scattering lengths it is impossible to distinguish all three pair correlation functions from one experiment alone. Hence the use of isotopes is imperative for a full understanding of this system, and has to be combined with a method of data analysis which derives the extent of orientational correlations between molecules, in order to extract a comprehensive picture of the short-range correlations between molecules.

The data open up many new avenues for investigation. For example it would now be appropriate to investigate the effect of temperature on these structures, and in fact probe the crystalline state as well to see the effect of melting on the orientational order. Given the unexpected ob-

servation of some antiparallel configurations occurring in the liquid, there is also now a clear need to develop a reliable intermolecular potential model, in order to test the present experimental data against computer simulation.

ACKNOWLEDGMENTS

The authors acknowledge the help of ISIS personnel in the execution of these experiments.

[1] C. Andreani, M. Nardone, F. P. Ricci, and A. K. Soper, Phys. Rev. A **46**, 4709 (1992).
[2] A. K. Soper, C. Andreani, and M. Nardone, Phys. Rev. E **47**, 2598 (1993).
[3] J. G. Powles, J. C. Dore, E. K. Osae, and J. H. Clarke, Mol. Phys. **44**, 1131 (1981).
[4] A. K. Soper and P. A. Egelstaff, Mol. Phys. **42**, 399 (1981).
[5] A. K. Soper, in *Advanced Neutron Sources 1988*, Proceedings of the International Collaboration on Advanced Neutron Sources-ICANS X, edited by D. K. Hyer, IOP Conf. Proc. No. 97 (Institute of Physics and Physical Society, Bristol, 1989), p. 353.
[6] A. K. Soper, W. S. Howells, and A. C. Hannon (unpublished).
[7] A. K. Soper, Nucl. Instrum. Methods **212**, 337 (1983).
[8] V. F. Sears, Neutron News **3**, 26 (1992).
[9] A. K. Soper and A. Luzar, J. Chem. Phys. **97**, 1320 (1992).
[10] P. Postorino, M. Nardone, M. A. Ricci, and M. Rovere, (unpublished).
[11] M. Cowan and W. Gordy, Phys. Rev. **111**, 209 (1958).
[12] *Comprehensive Inorganic Chemistry*, edited by A. F. Trotman-Dickenson (Pergamon, New York, 1973), Vol. 2, p. 1290.
[13] A. K. Soper, Chem. Phys. **107**, 61 (1986).
[14] A. K. Soper, *Neutron Scattering Data Analysis 1990*, Proceedings of the Workshop on Neutron Scattering Data Analysis, 1990, edited by M. W. Johnson, IOP Conf. Proc. No. 107 (Institute of Physics and Physical Society, Bristol, 1990), p. 57.
[15] C. G. Gray and K. E. Gubbins, *Fundamentals, Theory of Molecular Liquids,* Vol. 1 (Oxford University Press, New York, 1984).
[16] E. Sandor and R. F. Farrow, Nature **213**, 171 (1967); E. Sandor and M. W. Johnson, *ibid.* **217**, 541 (1968).
[17] A. K. Soper and M. G. Phillips, Chem. Phys. **107**, 47 (1986).

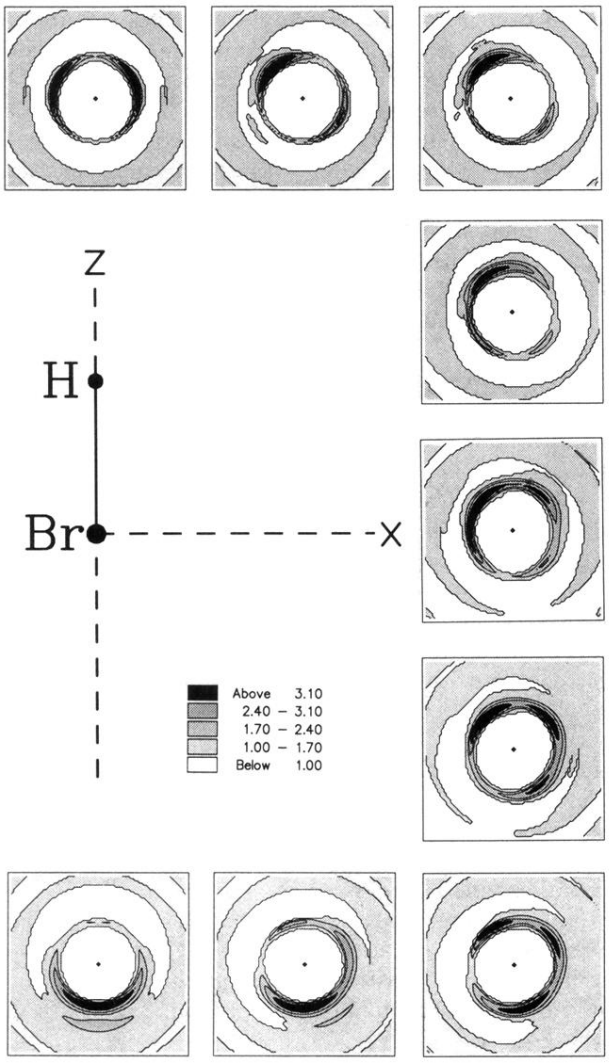

FIG. 7. Density maps of the angular pair correlation function between pairs of hydrogen-bromide molecules in the liquid state. A central molecule, molecule 1, is held fixed with its bromine atom at the origin of the laboratory coordinate system and with its hydrogen atom pointing along the positive z axis. Different directions away from this molecule are characterized by the value of θ_L, which is the angle made by molecular center-center vector with the z axis. The position of each map in the diagram, relative to the displayed coordinate system, corresponds closely to the actual value of θ_L for that map. Thus proceeding clockwise from the top the maps are shown for the different directions θ_L = 0°, 27°, 45°, 63°, 90°, 117°, 135°, 153°, and 180°. The maps are displayed on a square 20 Å× 20 Å. In each map the pair correlation function is shown as a function of the distance of a second molecule, molecule 2, from molecule 1 (central black dot). The angular variation of the intensity in each map corresponds to molecule 2 pointing in different directions in the x-z plane of the coordinate system relative to molecule 1. Dark regions in each map correspond to areas of enhanced density. For clarity, only values of the correlation function greater than unity are shown.